Iron-Mediated Oxidation of Methoxyhydroquinone under Dark Conditions: Kinetic and Mechanistic Insights

[Xiu Yuan](), [James A. Davis](), and [Peter S. Nico]()*

Earth and Environmental Sciences, Lawrence Berkeley National Laboratory, 1 Cyclotron Road, Berkeley, California 94720, United States

DOI: 10.1021/acs.est.5b03939

Publication Date (Web): January 20, 2016

Abstract

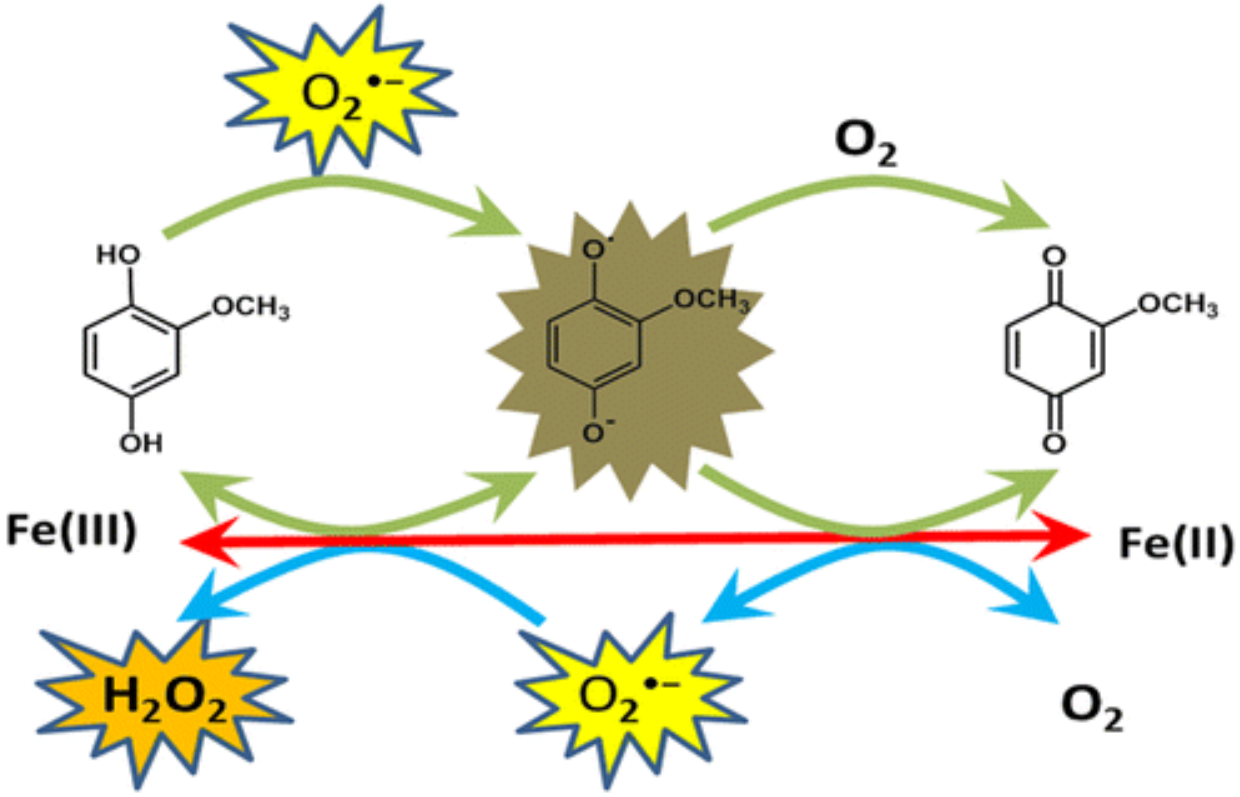

Despite the biogeochemical significance of the interactions between natural organic matter (NOM) and iron species, considerable uncertainty still remains as to the exact processes contributing to the rates and extents of complexation and redox reactions between these important and complex environmental components. Investigations on the reactivity of low-molecular-weight quinones, which are believed to be key redox active compounds within NOM, toward iron species, could provide considerable insight into the kinetics and mechanisms of reactions involving NOM and iron. In this study, the oxidation of 2-methoxyhydroquinone (MH_2Q) by ferric iron (Fe(III)) under dark conditions in the absence and presence of oxygen was investigated within a pH range of 4–6. Although Fe(III) was capable of stoichiometrically oxidizing MH_2Q under anaerobic conditions, catalytic oxidation of MH_2Q was observed in the presence of O_2 due to further cycling between oxygen, semiquinone

radicals, and iron species. A detailed kinetic model was developed to describe the predominant mechanisms, which indicated that both the undissociated and monodissociated anions of MH_2Q were kinetically active species toward Fe(III) reduction, with the monodissociated anion being the key species accounting for the pH dependence of the oxidation. The generated radical intermediates, namely semiquinone and superoxide, are of great importance in reaction-chain propagation. The kinetic model may provide critical insight into the underlying mechanisms of the thermodynamic and kinetic characteristics of metal–organic interactions and assist in understanding and predicting the factors controlling iron and organic matter transformation and bioavailability in aquatic systems.

1 Introduction

Natural organic matter (NOM), a chemically diverse mixture of heterogeneous organic compounds with various structural and functional properties, is ubiquitous in terrestrial and aquatic environments. Considerable attention has been drawn to the redox properties of NOM because of its great significance in a wide range of biogeochemical processes including iron bioreduction and contaminant transformation. The electron accepting and donating capacities of NOM have been attributed to the presence of redox-active constituents, such as quinone and phenolic functional groups.(1-4) Numerous studies also suggested that quinone moieties in NOM not only contribute to the reduction of organic contaminants, such as alkyl halides and nitroaromatics, but also stimulate the reduction of ferric oxides by iron-reducing bacteria.(3-9)

The term quinone collectively refers to organic structures in three oxidation states with one electron reduction of a quinone forming a semiquinone radical that can be further reduced to the hydroquinone form.(10) These species are common constituents of many biologically relevant molecules and serve as a vital link in the movement of electrons through cells and tissues.(8, 11-13) For example, oxidations of dihydroxybenzenes to benzoquinones and corresponding back-reactions are often reversible under neutral and acidic conditions, earning them a prominent place in organic electron-transfer chemistry. Furthermore, the frequently observed positive correlation between free radical concentrations in NOM and Fe(III) reduction using electron spin resonance (ESR) spectroscopy has been attributed to the existence of semiquinone radicals, a radical formed either from the one-electron oxidation of hydroquinones, the one-electron reduction of quinones, or the one-electron transfer from hydroquinones to quinones (a process termed “comproportionation”).

(1, 3, 13-15) Although commonly presented in very low concentrations due to its high reactivity, semiquinone radicals are kinetically important in the reversible redox chemistry of quinones. (9) Previous studies also indicated that quinone moieties are important electron-transfer groups in humic substances (HS) for both biotic and abiotic reduction and oxidation of HS.(1, 16) Besides, recent studies by Garg et al.(17, 18) reported that the occurrence of Fe(III) reduction by Suwanee River Fulvic Acid (SRFA, a proxy for terrestrial NOM), in nonirradiated acidic solutions was mainly attributed to the reduced hydroquinone-like moieties intrinsically presented in SRFA.(2, 4) Therefore, studies involving the redox behavior of quinones in metal reduction have important implications and may provide critical information regarding reaction mechanisms and functional groups that participate in the mobilization and immobilization of a variety of redox-sensitive metals in terrestrial and aquatic environments. For example, hydroquinone-mediated reduction of Fe(III) could increase the solubility and bioavailability of this critical trace element,(6) while quinone-mediated oxidation of uranium(IV) could affect its mobility and thus the remediation of contaminated sites.(5)

Iron, as a micronutrient in both aquatic and terrestrial ecosystems, is essential for virtually all life forms and plays a critical role in many biogeochemical processes. In natural waters, iron exists in two oxidation states, Fe(II) and Fe(III). Despite being more thermodynamically stable, Fe(III) quickly hydrolyzes and precipitates at circumneutral pH and thus becomes unavailable for direct biological uptake,(19) while the reduced form, Fe(II), is much more soluble and thus potentially more abundant in a bioavailable form.(17) However, in oxygenated waters, Fe(II) is rapidly oxidized to Fe(III) at circumneutral pH, which in turn limits its bioavailability. Despite the biogeochemical functioning of the equilibration and cycling of the Fe(II)–Fe(III) couple, fundamental insights into the control and dynamics of interconversion between Fe(II) and Fe(III) in natural waters are strictly limited, and how these processes restrict or enhance iron bioavailability are still largely unknown.

Quinones and iron likely coexist in the majority of the natural ecosystem, ranging from the surface water to groundwater and from soils to sediments. Because the highly complex nature of NOM could potentially interfere with efforts to explore the reactivity of quinone moieties on a molecular level, investigations of low-molecular-weight quinones could provide considerable insight into the thermodynamics, kinetics, and mechanisms of reactions involving quinone moieties.(20) Though there is a range of different quinone moieties presented in NOM, including benzoquinone-based compounds, such as sorgoleone, and naphthoquinone-based compounds, such as juglone and lawsone, as well as anthraquinone-based compounds,(20) a number of previous studies have indicated that those compounds are kinetically closely related to their redox potentials and functional groups, with the kinetic understanding of one providing a window to interpretation of associated

chemistry and biochemistry of the other.(8, 11, 14, 20-22) 2-Methoxyhydroquinone (MH_2Q; see abbreviations of different quinone species and detailed structure information in Figure S1), as an intermediate product during lignin degradation, is a common constituent of NOM and has the highest oxidoreductase activity among a series of low-molecular-weight quinones.(23, 24)This study, therefore, investigated the oxidation of MH_2Q by Fe(III) under both anaerobic and aerobic conditions over the pH range of 4–6, with emphasis on development of a rigorous kinetic description of the oxidation mechanism and insights on the role of free radicals, such as semiquinone and superoxide. Thermodynamic characteristics of this system were also discussed by employing the half-cell reduction potentials of different redox couples to verify modeled rate constants of the reactions involving quinone species. Acidic conditions were employed in this study partially to avoid complications associated with the precipitation of iron oxides, but they do reflect conditions of acid mine-drainage waters and coastal environments with the presence of acid sulfate soils.

2 Materials and Methods

A complete description of the materials and methods used is presented in section SI2.

2.1 Reagents

All solutions were prepared using 18 MΩ.cm ultrapure Milli-Q water (Thermo Fisher Scientific). Analytical grade chemicals were purchased from VWR International or Sigma-Aldrich (or as otherwise stated) and used without further refinement. Stock solutions were refrigerated at 4 °C in the dark when not in use. All studies were performed in 10 mM NaCl at a controlled room temperature of 22 ± 0.5 °C. Experiments were conducted in darkness with the reactor covered in foil for the duration of the reaction. Anaerobic data were collected in an anaerobic glovebag (Coy Laboratory Products, Grass Lake, MI) filled with 5% H_2 and 95% N_2. It is worth mentioning that all the anaerobic experiments conducted in the glovebox here were completed within 30 min, during which no interference from H_2 was observed. However, the slow reduction of 2-methoxybenzoquinone (MBQ) stock solution to MH_2Q during an overnight stay in the chamber (more than 17 h) was observed, suggesting that interference reduction from H_2 has to be considered for long-term experiments in the glovebox.

2.2 Experimental Measurements

Measurement of MBQ

Concentrations of MBQ were determined spectrophotometrically using a UV–vis spectrophotometer (Thermo Fisher Scientific) with $\varepsilon_{257} = 1.48 \times 10^4\ M^{-1}\ cm^{-1}$.

Fe(II) Determination

Concentrations of total Fe(II) were determined using a modified FZ method.(17)

H_2O_2 Determination

Previous studies(21, 22) indicated the potential interference from hydroquinones on H_2O_2detection using the fluorescence method;(25) therefore, a chemiluminescence-based method (the AE-CL method)(26) was employed for H_2O_2 measurement in this study.

2.3**Kinetic Modeling**

The kinetic model was fitted to the experimental data over a range of experimental conditions using the program Kintek Explorer.(27) The sensitivity of the model to changes in individual rate constant values was also assessed by examining the change in the relative difference between the experimental data and the kinetic model (defined as the relative residual, *r*) when one rate constant was varied while holding the others fixed at their optimal values. The program Kintecus(28) was employed to evaluate the kinetic model using a VBA program to calculate *r* (see the detailed description and Figure S3 in the Supporting Information).

3 Results and Discussion

3.1**Anaerobic Oxidation of MH_2Q by Fe(III)**

Previous studies have investigated the redox chemistry of hydroquinones and metal species in oxic environments,(17, 18, 21, 22, 29) but interaction involving these active components under dark anaerobic conditions is also of great interest, not only because such matrix composition better features the redox circumstances in anoxic environments (groundwater, deep ocean, sediments, et al.) but also the absence of O_2 allows full expression of the redox functions of metals and quinones and thus enables a thorough estimation of the generation of semiquinone radicals under dark anaerobic conditions. Furthermore, the reaction mechanism under anaerobic condition is an essential component for the complete kinetic description of the oxidation mechanism occurring in the presence of O_2. Therefore, in this study, the oxidation of MH_2Q by Fe(III) was first investigated under anaerobic conditions, with results shown in Figures 1, 2, S4, and S5). Precipitation of Fe(III) species in the system can be characterized as insignificant in these experiments for several reasons: (1) the acidic conditions that enable the existence of more soluble Fe(III) species, (2) the very low concentrations of Fe(III) employed here, and (3) evidence that >90% of added Fe(III) was quickly reduced to Fe(II) by MH_2Q before any significant nucleation/precipitation occurred (Figures 2, 4,

and S8; also see the detailed explanation in section SI4). Therefore, no further consideration was given to precipitation of Fe(III) in this study. Also, Fe(III) and Fe(II) were used as single entities to represent all ferric and ferrous species, respectively.

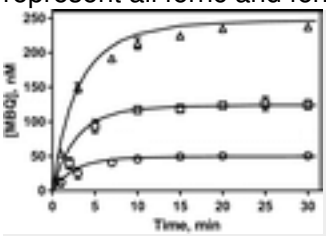

Figure 1. Anaerobic oxidation of 500 nM MH_2Q by Fe(III) at pH 5: (○) $[Fe(III)]_0$ = 100 nM, (□) $[Fe(III)]_0$ = 250 nM, and (△) $[Fe(III)]_0$ = 500 nM. Error bars (some of which are too small to be visible) are the standard errors from triplicate measurements, and solid lines represent the model fit using reactions 1–5 (Table 1).

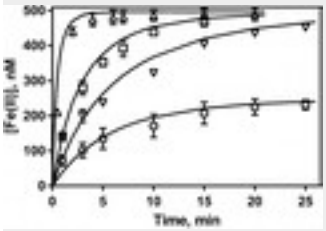

Figure 2. Generation of Fe(II) from anaerobic oxidation of MH_2Q by Fe(III) at different pH and $[MH_2Q]_0$ = 500 nM: (○) $[Fe(III)]_0$ = 250 nM at pH 4, (▽) $[Fe(III)]_0$ = 500 nM at pH 4, (□) $[Fe(III)]_0$ = 500 nM at pH 5, and (△) $[Fe(III)]_0$ = 500 nM at pH 6. Error bars (some of which are too small to be visible) are the standard errors from triplicate measurements, and solid lines represent the model fit using reactions 1–5 (Table 1).

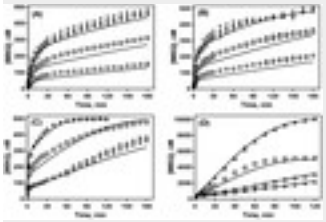

Figure 3. Aerobic oxidation of MH_2Q by Fe(III) at different pH. (A–C): $[MH_2Q]_0$ = 500 nM at (A) pH 4, (B) pH 5, and (C) pH 6 with (○) $[Fe(III)]_0$ = 100 nM, (□) $[Fe(III)]_0$ = 250 nM, and (△) $[Fe(III)]_0$ = 500 nM; (D): $[Fe(III)]_0$ = 500 nM at (◊) pH 4 with $[MH_2Q]_0$ = 5 μM, (○) pH 5 with $[MH_2Q]_0$ = 5 μM, (□) pH 6 with $[MH_2Q]_0$ = 5 μM, and (△) pH 6 with $[MH_2Q]_0$ = 10 μM. Error bars (some of which are too small to be visible) are the standard errors from triplicate measurements, and solid lines represent the model fit using reactions 1–9 (Table 1).

Figure 1 illustrates results for anaerobic oxidation of 500 nM MH_2Q by different concentrations of Fe(III) at pH 5. The steady-state concentrations of generated MBQ were proportional to added $[Fe(III)]_0$, with a specific ratio of 1:2. This is in accordance with previous studies(30-32) reporting that the overall stoichiometry for the oxidation of hydroquinone by Fe(III) is

$$MH_2Q + 2Fe(III) \xrightarrow{(-H^+),k_{anaerobic}} MBQ + 2Fe(II) \quad (1)$$ which could be further confirmed by Fe(II) generation profiles shown in Figure S6. At pH 5, while 500 nM Fe(III) was completely reduced to Fe(II) at t = 20 min, only ~250 nM of MBQ was generated. pH dependence of MH_2Q oxidation by Fe(III) was shown in Figure 2, as well as in Figures S4 and S5. The generation rate of Fe(II), as can be seen from Figure 2, increased significantly with increasing pH. For example, in the presence of 500 nM $[MH_2Q]_0$, 500 nM Fe(III) was completely reduced to Fe(II) within 5 min at pH 6, while less than 50% of Fe(III) was reduced within the same period at pH 4. Similar trends could also be observed in the generation rate of MBQ in Figure S4, which showed that 250 nM $[Fe(III)]_0$ was capable of oxidizing ~120 nM MH_2Q in the first 2 min at pH 6, but less than 20 nM MH_2Q was oxidized in the same duration at pH 4 (Figure S4 and similar behavior in Figure S5). The pH dependence of redox reactions between hydroquinones and ferric or cupric species has been previously observed and was interpreted in terms of reactions via different ionized forms of hydroquinones in various reaction routes.(21, 22, 33-37) While the monodissociated hydroquinone was postulated as the most kinetically active species toward the reduction of metal species,(8, 21, 38) studies by Rich and Bendall(35, 36)reported that the undissociated hydroquinone species could also contribute to the reduction of cytochrome *c* by hydroquinone at acidic pH, which is consistent with the conclusion from a recent study on copper-catalyzed oxidation of naphthohydroquinone.(22)

3.2 **Aerobic Oxidation of MH_2Q by Fe(III)**

The autoxidation of MH_2Q (autoxidation is oxidation in the absence of metal catalysts; see results in section SI6) was found to be negligibly slow under the conditions of this study, principally because of the lower pHs employed here and the high redox potential and p*K*a's possessed by MH_2Q,(8, 22) making the first electron transfer from MH_2Q to O_2 highly endergonic;(4) thus, this reaction was not further considered in this study. Fe(III)-mediated oxidation of MH_2Q in the presence of O_2 was inspected, with emphasis on the effects of pH, $[Fe(III)]_0$ and $[MH_2Q]_0$, as shown in Figure 3. First and foremost, unlike the results obtained under anaerobic conditions, nonstoichiometric oxidation, or in other words, catalytic oxidation of MH_2Q by Fe(III) was observed, especially in Figure 3D, which demonstrated that at pH 6, 500 nM Fe(III) was capable of completely oxidizing 10 μM MH_2Q within 2 h. Similar tests were also conducted on 1,4-benzohydroquinone, and no significant catalytic oxidation was found, presumably because the methoxy group substitution lowers the redox potential of the hydroquinone and makes it more facile for oxidation by Fe(III).(8) Because we already confirmed that direct oxidation of MH_2Q by O_2 is negligible in this system, the rapid oxidation of additional MH_2Q must occur, at least partially, with mediation of iron.

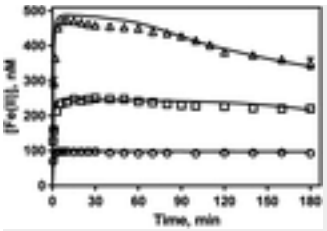

Figure 4. Generation of Fe(II) from aerobic oxidation of MH_2Q by Fe(III) at pH 6, $[MH_2Q]_0$ = 500 nM with (○) $[Fe(III)]_0$ = 100 nM, (□) $[Fe(III)]_0$ = 250 nM and (△) $[Fe(III)]_0$ = 500 nM. Error bars (some of which are too small to be visible) are the standard errors from triplicate measurements, and solid lines represent the model fit using reactions 1–9 (Table 1).

It is also noteworthy that Figure 3 showed that Fe(III) oxidizes MH_2Q to MBQ in a biphasic manner, with initial rapid formation of MBQ followed by a much slower increase in MBQ concentration over time. The initial concentration of MBQ that was rapidly formed was approximately linear-proportional to the added Fe(III) concentration (similar to anaerobic oxidation, where stoichiometric amount of MH_2Q was quickly oxidized by added Fe(III)) and thus was ascribed to direct oxidation of MH_2Q by added Fe(III). This could be further justified by Figure 4and Figure S8 showing Fe(III) was nearly completely reduced to Fe(II) by the end of the initial rapid phase of oxidation, indicating the direct oxidation of MH_2Q by Fe(III) is rapid and not rate-limiting. Instead, the following much slower process, involving multiple O_2-mediated reactions, such as the regeneration of Fe(III) by oxidizing Fe(II) at such acidic pH,(39, 40) might be more rate-determining in the overall oxidation. However, it is interesting to notice that in Figure 3, the rate of oxidation is not only correlated with the Fe(III) concentration but also increased with increasing the initial concentration of the hydroquinone ($[MH_2Q]_0$, Figure S9), similar to behavior observed in a previous study on copper-mediated oxidation of naphthohydroquinone.(22) More specifically, as shown in Figure 3D, at pH 6, more MH_2Q was oxidized per unit of time when $[MH_2Q]_0$ = 10 μM than that with $[MH_2Q]_0$ = 5 μM; similarly, a comparison between Figures 3A–C and Figure 3D indicates that at each pH with $[Fe(III)]_0$ = 500 nM, much more MH_2Q was oxidized per unit of time when $[MH_2Q]_0$ = 5 μM than that with $[MH_2Q]_0$ = 500 nM. This was especially observed within the second oxidation phase, indicating that iron-mediated reactions might not be the only factor dominating the “slow oxidation phase”, and instead MH_2Q-involved processes must also play a role. Nevertheless, as we declared that the direct interaction between MH_2Q and Fe(III) is rapid and thus not likely to be rate limiting, other reactions involving intermediates generated from MH_2Q-dependent activities, most likely the semiquinone radicals,(21, 22) might be more important in determining the slow oxidation rate.

Similar to anaerobic oxidation, there is also apparent pH dependence of the aerobic oxidation of MH_2Q by Fe(III) (as shown in Figure 3 and Figure S7), i.e., the overall oxidation rate increased with increasing pH from 4 to 6, and such dependence was observed in both oxidation phases (the initial rapid phase and the later slow phase). Apparently, the mechanism accounting for the anaerobic pH dependence (involvement of different ionized forms of MH_2Q in reactions with ferric species) is inevitably contributing here, but other pH sensitive processes, such as the oxidation of Fe(II) by dioxygen and superoxide,(19, 39, 40) could also impact the overall pH dependence.

Besides the generation of MBQ, the transformation of iron in the system is also of great interest. Direct measurement of Fe(II) concentrations over a range of conditions was undertaken to assist in determining the mechanism and constraining the fitting parameters. The corresponding results are shown in Figure 4 and Figure S8. Within the pH range 4–6, all of Fe(III) added to 500 nM MH_2Q solution was quickly reduced to Fe(II), with the reduction rate increasing with increase in pH. As for pH 4 (Figure S8), the concentration of Fe(II) reached its maximum level after more than 30 min of the reaction initiation, while at pH 6, the highest concentration was quickly achieved within 7 min (Figure 4). Alhough the reoxidation of Fe(II) to Fe(III) was happening concurrently,(19, 39, 40) this reaction was too slow to compete against the rapid reduction of Fe(III) to Fe(II) by MH_2Q. This is to say, all of the Fe(III) regenerated from the oxidation of Fe(II) by O_2 and other oxidants (such as superoxide and semiquinone radicals; see detailed mechanism in next section and in Table 1) was immediately rereduced to Fe(II) by MH_2Q; thus, almost all of the iron was observed as Fe(II) in the system in spite of the predominating oxygenated conditions. The cycling between Fe(III) and Fe(II) kept proceeding until MH_2Q was totally consumed and, subsequently, the concentration of Fe(II) started to decline simply because of the oxygenation of Fe(II) to Fe(III). This is clearly the case demonstrated in Figure 4, with the top curve representing the reduction of 500 nM Fe(III) by 500 nM MH_2Q at pH 6. After the pseudoequilibrium between Fe(II) and Fe(III) (8–60 min), the obvious decrease of [Fe(II)] began at $\sim t = 60$ min, at which point the added 500 nM of MH_2Q was nearly completely transformed to MBQ (Figure 3C).

Table 1. Modeled Reactions and Rate Constants of MH_2Q Oxidation by Fe(III)

no.	reaction	rate constant/$M^{-1} \cdot s^{-1}$[a]	reference
1	$MH_2Q^0 \rightleftharpoons MHQ^- + H^+$	$K_{a1} = 10^{-9.91}$ M	(20, 49)

no.	reaction	rate constant/$M^{-1} \cdot s^{-1}$[a]	reference
2	$MHQ^- \rightleftharpoons MQ^{2-} + H^+$	$K_{a2} = 10^{-11.9}$ M	(20, 49)
3	$MH_2Q^0 + Fe(III) \underset{(+H^+),k_{-3}}{\overset{(-H^+),k_3}{\rightleftharpoons}} Fe(II) + MSQ^{\bullet}$	$k_3 = (2.4 \pm 0.4) \times 10^3$ $k_{-3} = 1.0 \times 10^5$	This study(17, 18, 29)
4	$MHQ^- + Fe(III) \underset{(+H^+),k_{-3}}{\overset{(-H^+),k_4}{\rightleftharpoons}} Fe(II) + MSQ^{\bullet}$	$k_4 = (3.0 \pm 0.4) \times 10^8$ $k_{-3} = 1.0 \times 10^5$	This study(17, 18, 29)
5	$Fe(III) + MSQ^{\bullet -} \xrightarrow{k_5} Fe(II) + MBQ$	$k_5 = (1.2 \pm 0.3) \times 10^7$	This study
6	$MSQ^{\bullet -} + O_2 \underset{k_{-6}}{\overset{k_6}{\rightleftharpoons}} MBQ + O_2^{\bullet -}$	$k_6 = 1.5 \times 10^6$ $k_{-6} = 3.3 \times 10^8$	(8, 50)
7	$MH_2Q + O_2^{\bullet -} \xrightarrow{k_7} MSQ^{\bullet -} + H_2O_2$	$k_7 = 7.0 \times 10^5$	This study
		pH 4 5 6	
8	$Fe(II) + O_2 \underset{k_{-8}}{\overset{k_8}{\rightleftharpoons}} Fe(III) + O_2^{\bullet -}$	k_8 1.3×10^{-4} 1.3×10^{-3} 1.3×10^{-2}	(19, 51, 39, 52-54)

no.	reaction	rate constant/$M^{-1} \cdot s^{-1}$[a]	reference
		k_{-8} 6.8×10^6 3.1×10^7 1.5×10^8	
9	$Fe(II) + O_2^{\bullet -} \xrightarrow{k_9} Fe(III) + H_2O_2$	k_9 2.4×10^6 6.6×10^6 1.0×10^7	

a
Unless noted otherwise.

To gain some insight into the Fe(III)–Fe(II) transformation in the system, we have calculated the cycling rate and the turnover frequency of iron using a modified version of the kinetic model reported in Table 1, with detailed description and results provided in section SI7 (Figures S12 and S13). As an example, for the case of 500 nM Fe(III) and 10 μM MH_2Q at pH 6, cycling between Fe(III) and Fe(II) occurs at the very beginning of the reaction, with a turnover frequency of ∼6 h^{-1}. By examining the contribution of different oxidants on the oxidation of MH_2Q (Figure S13), it is clear that besides Fe(III)–Fe(II), the O_2–$O_2^{\bullet-}$ couple, which oxidized almost 40% of MH_2Q, is another significant force driving the overall oxidation. This also explains the occurrence of nonstoichiometric oxidation of MH_2Q by Fe(III) in the presence of O_2. The additional MH_2Q was oxidized not only by the regenerated Fe(III) that resulted from oxidation of Fe(II) but also by direct reaction with $O_2^{\bullet-}$, generated either from reduction of O_2 by semiquinone or by Fe(II) (reactions 6 and 8, respectively; Table 1).

Previous studies also suggested that during the metal-catalyzed oxidation of hydroquinones, stoichiometric amounts of hydrogen peroxide (H_2O_2) would be generated.(8, 22, 41-44) H_2O_2 is of particular interest because of its ubiquitousness both in the cells of organisms as a byproduct of oxygen metabolism and in surface seawaters primarily due to photochemical processes mediated by NOM.(45) A recent study by Murphy et al.(46) also reported rapid production of H_2O_2 (with maximum concentrations of 3.85 μM) when anoxic groundwater mixed with oxidized, iron-rich sediments, indicating a metal redox cycling mechanism under dark conditions. More importantly, in the presence of iron, H_2O_2 may lead to the formation of highly reactive and damaging oxidants such as hydroxyl radical ($HO^{\bullet}$), a radical that is always present in vanishingly small concentration but will, in turn, induce the oxidation of both NOM and anthropogenic contaminants.(46-48)Therefore, the generation

of H_2O_2 during the oxidation of MH_2Q by Fe(III) at different pH values was also investigated, with results shown in Figure 5. Apparently, the rate of H_2O_2 generation, similar to the oxidation of MH_2Q, also exhibited strong pH dependence, with more rapid H_2O_2generated at pH 6 than at pH 4.

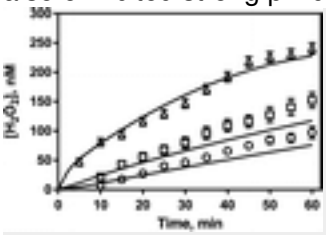

Figure 5. Generation of H_2O_2 from aerobic oxidation of MH_2Q by Fe(III) at different pH, $[MH_2Q]_0$ = 500 nM, and $[Fe(III)]_0$ = 500 nM at (○) pH 4, (□) pH 5, and (△) pH 6. Error bars (some of which are too small to be visible) are the standard errors from triplicate measurements, and solid lines represent the model fit using reactions 1–9 (Table 1).

3.3 **Kinetic Modeling of MH_2Q Oxidation by Fe(III)**

Because the dissociation states of a hydroquinone is of key importance for its electron-donating capability, the protonation–deprotonation reactions of MH_2Q were included in the model as reactions 1 and 2 in Table 1, with previously reported ionization constants.(20, 49) Under anaerobic conditions, the oxidation of MH_2Q by Fe(III) occurs via direct interactions between Fe(III) and hydroquinone species, and both the undissociated and monodissociated hydroquinones have been reported to be active toward reduction of ferric species, as expressed by reactions 3 and 4 in Table 1.(34, 36) Although the doubly dissociated species MQ^{2-} is thermodynamically more reactive, its reaction with Fe(III) is negligible in this study, considering its extremely low concentration (10^{-16}–10^{-20} M, from pH 6 to 4 under conditions of this study) and thus was not included in the model. The intermediate generated from one electron oxidation of the hydroquinone, the semiquinone radical, has been widely proposed to be inevitably involved in the pool with both oxidizing and reducing capibilities.(8, 18, 21, 34-37) Therefore, the reduction of Fe(III) by 2-methoxysemiquinone radical ($MSQ^{\bullet-}$) was included in the model as reaction 5, as well as the oxidation of Fe(II) by $MSQ^{\bullet-}$ (the back-reaction of reactions 3 and 4) with a reported rate of 1×10^5 $M^{-1}\cdot s^{-1}$ in recent studies by Garg et al.(17, 18, 29) on iron redox transformations in the presence of natural organic matter.

When O_2 is present, in addition to those reactions occurring anaerobically, reactions describing the electron transfers between oxygen and semiquinone radical, between superoxide and quinone species, as well as reactions depicting the oxidation of Fe(II), must also be included. The additional reactions included in the model due to the presence of O_2 with corresponding rate constants are listed as reactions 6–9 in Table 1. As previously stated, the autoxidation of MH_2Q is negligibly slow

under conditions of this study and thus was not required in the model. Because O_2has no charge, the Marcus theory of electron transfer predicts that rate constants for the reaction of semiquinone radical with O_2 will be a function of change in the Gibbs free energy.(8, 15) It has also been reported that for quinones with a standard midpoint potential of E^0(quinone–semiquinone) ≥ –150 mV, rate constants for the forward reactions follow well the Marcus theory for electron transfer and can be estimated by a reported linear relationship.(8, 36, 50) On the basis of this and E^0(MBQ–MSQ$^{\bullet-}$) = –0.017 V (see detailed calculations in section SI8), we estimated that the rate constant for the forward reaction was k_6 = 1.5 × 10^6 M^{-1}·s^{-1}. The equilibrium constant (K) of reaction 6 can also be determined by the standard reduction potential of both redox couples (MBQ–MSQ$^{\bullet-}$ and O_2–$O_2^{\bullet-}$) using the Nernst equation:(55) $$E^0_{(O_2-O_2^{\bullet-})} - E^0_{(MBQ-MSQ^{\bullet-})} = \frac{RT}{nF}\ln K$$ (2)where R is the gas constant in appropriate units, 8.314 J K^{-1} mol^{-1}. T is the temperature in Kelvin, F is the Faraday constant (9.6485 × 10^4 C mol^{-1}), and n is the number of electrons involved in the reaction. Thus, when n = 1, at 25 °C, eq 2 can be written as $$\log K = \frac{E^0_{(O_2-O_2^{\bullet-})} - E^0_{(MBQ-MSQ^{\bullet-})}}{0.059}$$ (3)Here, we employed the values of E^0(O_2–$O_2^{\bullet-}$) = –0.155 V(56-58) and E^0(MBQ–MSQ$^{\bullet-}$) = –0.017 V in eq 3 to calculate K_6 = 4.58 × 10^{-3}; thus, k_{-6} = k_6/K_6 = 3.3 × 10^8 M^{-1}·s^{-1}. These values agree very well with previous reported rate constants of methyl-hydroquinone (k_6 = 1.2 × 10^6 M^{-1}·$s^{-1}$and k_{-6} = 7.3 × 10^8 M^{-1}·s^{-1}),(50) which has close redox potentials to MH_2Q. Further, because of the substituent effect, the redox potential of MH_2Q lies between that of 1,4-benzohydroquinone and 1,4-naphthohydroquinone, both the forward- and reverse-rate constants of reaction 6 are also between these two analogous aromatics,(21, 22) which again confirms that the redox potential of the quinone–semiquinone couple governs the reaction of semiquinone with dioxygen to form superoxide.(8)

The comproportionation reaction between MH_2Q and MBQ was not important in the system as a result of the extremely low concentrations of the doubly dissociated hydroquinone species (MQ^{2-}, the well-established dominant active species toward comproportionation reaction,(15, 34, 36, 49)having a concentration of ∼10^{-16}–10^{-20} M from pH 6 to 4 under conditions of this study). Because MSQ$^{\bullet-}$ can be both oxidizing and reducing, it will readily disproportionate to corresponding hydroquinone and quinone. However, due to its low concentration and its rapid removal by dioxygen and iron species (reactions 3–6, Table 1), the disproportionation of MSQ$^{\bullet-}$ plays no significant role here. This could be further verified by the result that inclusion of these two reactions in the kinetic model with varying rate constants from 10–10^{10} M^{-1}·s^{-1} has no observable effect on the overall model fitting (Figure S3G and H). Therefore, these two reactions were not included in the model.

The oxidation of MH_2Q by superoxide, which was expected to have a relatively low reaction rate, (58) was included in the model as reaction 7. Previous studies(58-60) also suggested that reactions involving H_2O_2 in this system (such as the backward reaction of reaction 7; Table 1) were not important, presumably because the reaction rate between H_2O_2 and semiquinones ($\sim 10^4$– 10^5 $M^{-1}\cdot s^{-1}$) is low.(61, 62) Therefore, this reaction is unlikely to compete effectively with the rapid removal of semiquinones by dioxygen (reaction 6, Table 1). Further evidence for this was given by the sensitivity analysis, which demonstrated that inclusion of this reaction in the kinetic model and varying the rate constant from 10–10^5 $M^{-1}\cdot s^{-1}$ had negligible effect on the model fitting (see Figure S3I). As such, this reaction was excluded from the model. The disproportionation of $O_2^{\cdot-}$, with rates of 6×10^6 and 6×10^8 $M^{-1}\cdot s^{-1}$ at pH 6 and 4, respectively,(63, 64) was not important here because of its low concentration and rapid reaction with iron and quinone species (reactions 6–9 in Table 1). This was also confirmed by the sensitivity analysis (see Figure S3J). Cross-dismutation between $MSQ^{\cdot-}$ and $O_2^{\cdot-}$ might also occur, but little information on this reaction has been previously reported and the rate constant is not known. Inclusion of this reaction in simulations and varying the rate constant over a reasonable range revealed minimal effect on the fitting (Figure S3K), justifying exclusion of this reaction from the model. The oxidation of Fe(II) (reactions 8 and 9), as the key route for regeneration of Fe(III) in the presence of O_2, has been extensively investigated at acidic and circumneutral pHs. Therefore, here we employed the well-established pH-dependent rates from previous studies(19, 39, 40, 51-54) for interactions between O_2, Fe(II)–Fe(III), and $O_2^{\cdot-}$.

Due to the limited information available in the literature, rate constants for the interactions of Fe(III) and quinone species (reactions 3, 4, and 5, Table 1) and the reaction between MH_2Q and $O_2^{\cdot-}$ (reaction 7, Table 1) were determined empirically by best fit of the model to the experimental data. Results of model fitting over the pH range 4–6 using reactions 1–9 (Table 1) are illustrated in Figures 1–5 (and Figures S4–S9). In general, the model provides reasonable fits to the experimental data over a range of conditions. The good agreement between the model output and the experimental data validates our assumptions of the proposed mechanism and the assignment of individual rate constants.

In accordance with previous studies,(34-36) both the undissociated and singly dissociated MH_2Q species (MH_2Q^0 and MHQ^-) were found to be kinetically active toward Fe(III) reduction, with intrinsic rate constants of 2.4×10^3 and 3.0×10^8 $M^{-1}\cdot s^{-1}$, respectively. Because the standard one-electron reduction potential of the $MSQ^{\cdot-}$–MH_2Q^0 couple is much higher than that of the $MSQ^{\cdot-}$–MHQ^- couple (see detailed calculations in section SI8), reaction 3 is less favorable in a thermodynamic sense and occurs via a rather slower rate than that of reaction 4. This again confirms that the monodissociated

hydroquinone anion is a substantially more facile electron donor to ferric species.(8, 34, 36) Although MHQ^- only occupies a small fraction of the total hydroquinone species at acidic pH, the protonation–deprotonation equilibrium is faster than that of redox reactions and thus is not rate-limiting.(35, 65) It is also worth mentioning that, although thermodynamically less favorable, reaction 3 is still feasible. We can conclude here that the back reaction is more rapid than the forward reaction because the rate of reaction between Fe(II) and semiquinone radical is almost 2 orders of magnitude higher than that of the forward reaction. Moreover, the rapid removal of the product, $MSQ^{\bullet-}$, by Fe(III) and O_2 (reactions 5 and 6, respectively) is another significant force driving the oxidation reaction to the right.(8, 35) Thus, the presence of O_2 in the system not only promotes Fe(III) resupply by continuously oxidizing Fe(II) but also induces the rapid removal of $MSQ^{\bullet-}$ with resultant generation of $O_2^{\bullet-}$. The model also indicates that the rate of $MSQ^{\bullet-}$ removal by O_2 > rate of removal by Fe(III) > rate of removal by Fe(II) > rate of removal by disproportionation, consistent with previously reported conclusion.(36)However, unlike the study by Uchimiya and Stone,(11) there is no back-reduction of MBQ by Fe(II) observed in this study, presumably due to the acidic pH and low concentrations of both reactants employed in this study.

The model predicted rate of 1.2×10^7 $M^{-1}{\cdot}s^{-1}$ for reduction of Fe(III) by $MSQ^{\bullet-}$ (reaction 5, Table 1) is higher than the value of 2×10^6 $M^{-1}{\cdot}s^{-1}$ reported by Yamazaki and Ohnishi(34) on the reduction of ferricytochrome *c* by semiquinones but lower than the value of 2×10^7 $M^{-1}{\cdot}s^{-1}$reported in a recent study on the reduction of cupric species by 1,4-semiquinone.(21)Furthermore, $MSQ^{\bullet-}$, with a standard one-electron reduction potential of $E^0(MBQ/MSQ^{\bullet-}) = -0.017$ V, is more reducing than oxidizing. This is to say, in a system with both Fe(III) and Fe(II) present, instead of shifting back to MH_2Q by oxidizing Fe(II), $MSQ^{\bullet-}$ is more likely to transfer to MBQ by reducing Fe(III), consolidating the model predicted $k_5 > k_{-3}$. As indicated in the study by Eyer,(58) the oxidation of MH_2Q by superoxide, was expected to have a relatively low reaction rate of $\sim 10^4$–10^5 $M^{-1}{\cdot}s^{-1}$.(66-68) Our model predicted rate of 7×10^5 $M^{-1}{\cdot}s^{-1}$ is also close to the value of 2×10^5 $M^{-1}{\cdot}s^{-1}$ reported in recent studies by Garg et al.(17) on iron redox transformations in the presence of NOM under acid conditions.

Despite the capability of the kinetic model in providing a good description of the various reactions between the quinone triad (MBQ, $MSQ^{\bullet-}$ and MH_2Q), Fe(III)–Fe(II), and O_2 over a range of experimental conditions with a relatively well-constrained set of rate constants, the model is limited by the assumption that the composite terms Fe(II) and Fe(III) adequately represent all inorganic iron in their +2 and +3 oxidation states, respectively. Therefore, care must be taken when interpreting the model results, because the model is condition-specific by default. For example, the presence of

complexing organic ligands would influence the reactivity of various iron species and as such the composite “intrinsic” rate constants of various reactions with iron will need to be re-evaluated.

3.4 Implication of Findings

In this study, we investigated the oxidation of MH_2Q by Fe(III) under dark conditions in the absence and presence of oxygen. Although Fe(III) was capable of stoichiometrically oxidizing MH_2Q under anaerobic conditions, catalytic oxidation of MH_2Q was observed in the presence of O_2 due to further cycling between iron, oxygen, and semiquinone radicals. Based on the experimental observations, a detailed kinetic model was developed to describe the predominant mechanisms operating in this system and to provide insights into the observed pH dependence and the role of generated radical intermediates. Our results also showed that the direct oxidation of MH_2Q by O_2 is spin-restricted and very slow under conditions of this study, but the Fe(III)/Fe(II) couple could overcome such restriction and perform as an electron-transfer agent between the hydroquinone and O_2 (similar to previous observed behaviors of copper species),(21, 22) leading to the existence of pseudostable but high concentrations of reduced Fe(II) under oxic and dark conditions that could potentially promote the generation of ROS. One particular example in this study is that the generation of $O_2^{\bullet-}$ and H_2O_2 from the redox cycling of iron between its +3 and +2 oxidation states in the presence of MH_2Q and O_2 confirms the essential role of NOM and reduced metals in nonphotochemical pathway for ROS formation in natural aquatic environments,(69)which, at the same time, are particularly important for the oxidative degradation of NOM itself and any further cascade of radical-promoted reactions with other constituents in natural waters.

Although the presence of O_2 is imperative for iron cycling and chain propagating to reach catalytic oxidation of MH_2Q in this study, in deep oceans and lakes and groundwater, where O_2 deficiency prevails, other components presented in such anoxic and anaerobic environments could serve to bridge Fe(II) and Fe(III) and thus facilitate iron cycling and further redox of quinones and NOM. For instance, Uchimiya and Stone(11) reported the oxidation of Fe(II) by various quinones at circumneutral pH could serve as a vital link in networks of electron transport in suboxic and anoxic environments. Studies also showed that chromium(VI) and manganese(III, IV) (hydr)oxides were capable of oxidizing Fe(II) under anoxic conditions.(70, 71) At the same time, the presence of fluctuating redox conditions and (micro)biological communities may also contribute, especially in low pH environments.(72) Therefore, the coexistence of quinones and iron could potentially facilitate the redox cycling of both species in allowable environments, and, separately or in concert, iron species (both dissolved and precipitated) and quinones are believed to be pivotal participants in a wide range of environmental redox reactions.

Due to the close correlations between kinetic and thermodynamic characteristics of quinone triads and their structures and functional groups, the kinetic model and associated rate constants reported in this study could provide insight into the rate and extent of interactions between other quinone members and metals that have different electrophilicity and redox potentials. However, although quinone moieties are recognized to dominate the redox properties of NOM, care must be taken when interpreting the results observed in pure quinone solutions to the natural aquatic environment, where the presence of an extended network of complexing organic ligands would influence the reactivity of various iron species and the stability of radicals. For example, similarities and differences in iron redox transformations between a simple quinone and the quinone moieties presented in SRFA were identified in recent studies by Jiang et al.(73) and Garg et al.,(18) where increased stability of semiquinone radicals were found in SRFA solution compared to that in pure hydroquinone solution, indicating quinone moieties presented in highly conjugated and substituted environment of NOM will play a much more important role in the rate and extent of metal redox transformations.

Supporting Information

The Supporting Information is available free of charge on the ACS Publications website at DOI: 10.1021/acs.est.5b03939.

- Additional detailed information on the structures of 2-methoxybenzoquinone triad, experimental methods, manipulative experiments, sensitivity analysis and extra experimental data and calculations. (PDF)

- **PDF**
  - es5b03939_si_001.pdf (865.64 kB)

Iron-Mediated Oxidation of Methoxyhydroquinone under Dark Conditions: Kinetic and Mechanistic Insights

figshare

ShareDownload

The authors declare no competing financial interest.

Acknowledgment

The work reported here is supported as part of the Sustainable Systems (SS) Scientific Focus Area (SFA) program at LBNL, funded by the U.S. Department of Energy, Office of Science, Office of Biological and Environmental Research, Subsurface Biogeochemical Research Program, under award number DE-AC02-05CH11231. The authors gratefully acknowledge the assistance from Dr. Christopher Miller at the University of New South Wales (Australia) for the model sensitivity calculations.

- Reference QuickView

References

This article references 73 other publications.

1. 1.

   Scott, D. T.; McKnight, D. M.; Blunt-Harris, E. L.; Kolesar, S. E.; Lovley, D. R. Quinone moieties act as electron acceptors in the reduction of humic substances by humics-reducing microorganisms *Environ. Sci. Technol.* **1998**, 32 (19) 2984– 2989 DOI: 10.1021/es980272q

   [ACS Full Text], [CAS]

2. 2.

   Aeschbacher, M.; Graf, C.; Schwarzenbach, R. P.; Sander, M. Antioxidant properties of humic substances*Environ. Sci. Technol.* **2012**, 46 (9) 4916– 4925 DOI: 10.1021/es300039h

   [ACS Full Text], [CAS]

3. 3.

   Nurmi, J. T.; Tratnyek, P. G. Electrochemical Properties of Natural Organic Matter (NOM), Fractions of NOM, and Model Biogeochemical Electron Shuttles *Environ. Sci. Technol.* **2002**, 36 (4) 617– 624 DOI: 10.1021/es0110731

   [ACS Full Text], [CAS]

4. 4.

Aeschbacher, M.; Sander, M.; Schwarzenbach, R. P. Novel electrochemical approach to assess the redox properties of humic substances *Environ. Sci. Technol.* **2010**, 44 (1) 87– 93 DOI: 10.1021/es902627p

[ACS Full Text], [CAS]

5. 5.

Chen, J.; Gu, B.; Royer, R. A.; Burgos, W. D. The roles of natural organic matter in chemical and microbial reduction of ferric iron *Sci. Total Environ.* **2003**, 307 (1–3) 167– 178 DOI: 10.1016/S0048-9697(02)00538-7

[Crossref], [PubMed], [CAS]

6. 6.

Lovley, D. R.; Coates, J. D.; Blunt-Harris, E. L.; Phillips, E. J.; Woodward, J. C. Humic substances as electron acceptors for microbial respiration *Nature* **1996**, 382 (6590) 445– 448 DOI: 10.1038/382445a0

[Crossref], [CAS]

7. 7.

Lovley, D. R.; Woodward, J. C.; Chapelle, F. Stimulated anoxic biodégradation of aromatic hydrocarbons using Fe (in) ligands *Nature* **1994**, 370, 128– 131 DOI: 10.1038/370128a0

[Crossref], [PubMed], [CAS]

8. 8.

Song, Y.; Buettner, G. R. Thermodynamic and kinetic considerations for the reaction of semiquinone radicals to form superoxide and hydrogen peroxide *Free Radical Biol. Med.* **2010**, 49 (6) 919– 962 DOI: 10.1016/j.freeradbiomed.2010.05.009

[Crossref], [PubMed], [CAS]

9. 9.

Uchimiya, M.; Stone, A. T. Reversible redox chemistry of quinones: Impact on biogeochemical cycles*Chemosphere* **2009**, 77 (4) 451– 458 DOI: 10.1016/j.chemosphere.2009.07.025

[Crossref], [PubMed], [CAS]

10. 10.

Laviron, E. Electrochemical reactions with protonations at equilibrium: Part VIII. The 2*e*, $2H^+$ reaction (nine-member square scheme) for a surface or for a heterogeneous reaction in the absence of disproportionation and dimerization reactions *J. Electroanal. Chem. Interfacial Electrochem.* **1983**, 146 (1) 15– 36 DOI: 10.1016/S0022-0728(83)80110-7

[Crossref], [CAS]

11. 11.

Uchimiya, M.; Stone, A. T. Reduction of substituted p-benzoquinones by Fe II near neutral pH *Aquat. Geochem.* **2010**, 16 (1) 173– 188 DOI: 10.1007/s10498-009-9077-0

[Crossref], [CAS]

12. 12.

Hong, Y.; Sengupta, S.; Hur, W.; Sim, T. Identification of Novel ROS Inducers: Quinone Derivatives Tethered to Long Hydrocarbon Chains *J. Med. Chem.* **2015**, 58 (9) 3739– 3750 DOI: 10.1021/jm501846y

[ACS Full Text], [CAS]

13. 13.

Paul, A.; Stösser, R.; Zehl, A.; Zwirnmann, E.; Vogt, R. D.; Steinberg, C. E. W. Nature and abundance of organic radicals in natural organic matter: Effect of pH and irradiation *Environ. Sci. Technol.* **2006**, 40 (19)5897– 5903 DOI: 10.1021/es060742d

[ACS Full Text], [CAS]

14. 14.

Uchimiya, M.; Stone, A. T. Redox reactions between iron and quinones: Thermodynamic constraints*Geochim. Cosmochim. Acta* **2006**, 70 (6) 1388– 1401 DOI: 10.1016/j.gca.2005.11.020

[Crossref], [CAS]

15. 15.

Roginsky, V.; Pisarenko, L. M.; Bors, W.; Michel, C. The kinetics and thermodynamics of quinone-semiquinone-hydroquinone systems under physiological conditions *J. Chem. Soc., Perkin Trans. 2* **1999**, 4)871– 876 DOI: 10.1039/a807650b

[Crossref], [CAS]

16. 16.

Aeschbacher, M.; Vergari, D.; Schwarzenbach, R. P.; Sander, M. Electrochemical analysis of proton and electron transfer equilibria of the reducible moieties in humic acids *Environ. Sci. Technol.* **2011**, 45 (19)8385– 8394 DOI: 10.1021/es201981g

[ACS Full Text], [CAS]

17. 17.

Garg, S.; Ito, H.; Rose, A. L.; Waite, T. D. Mechanism and kinetics of dark iron redox transformations in previously photolyzed acidic natural organic matter solutions *Environ. Sci. Technol.* **2013**, 47 (4) 1861– 1869DOI: 10.1021/es3035889

[ACS Full Text], [CAS]

18. 18.

Garg, S.; Jiang, C.; David Waite, T. Mechanistic insights into iron redox transformations in the presence of natural organic matter: Impact of pH and light *Geochim. Cosmochim. Acta* **2015**, 165, 14– 34 DOI: 10.1016/j.gca.2015.05.010

[Crossref], [CAS]

19. 19.

Pham, A. N.; Waite, T. D. Oxygenation of Fe(II) in natural waters revisited: Kinetic modeling approaches, rate constant estimation and the importance of various reaction pathways *Geochim. Cosmochim. Acta* **2008**,72 (15) 3616– 3630 DOI: 10.1016/j.gca.2008.05.032

[Crossref], [CAS]

20. 20.

Uchimiya, M.; Stone, A. T. Aqueous oxidation of substituted dihydroxybenzenes by substituted benzoquinones *Environ. Sci. Technol.* **2006**, 40 (11) 3515– 3521 DOI: 10.1021/es052578k

[ACS Full Text], [CAS]

21. 21.

Yuan, X.; Pham, A. N.; Miller, C. J.; Waite, T. D. Copper-catalyzed hydroquinone oxidation and associated redox cycling of copper under conditions typical of natural saline waters *Environ. Sci. Technol.* **2013**, 47 (15)8355– 8364 DOI: 10.1021/es4014344

[ACS Full Text], [CAS]

22. 22.

Yuan, X.; Miller, C. J.; Pham, A. N.; Waite, T. D. Kinetics and mechanism of auto- and copper-catalyzed oxidation of 1,4-naphthohydroquinone *Free Radical Biol. Med.* **2014**, 71 (0) 291– 302 DOI: 10.1016/j.freeradbiomed.2014.03.021

[Crossref], [PubMed], [CAS]

23. 23.

Kirk, T. K.; Lorenz, L. F. Methoxyhydroquinone, an Intermediate of Vanillate Catabolism by Polyporus dichrous *Appl. Microbiol.* **1973**, 26 (2) 173– 175

[PubMed], [CAS]

24. 24.

Buswell, J. A.; Hamp, S.; Eriksson, K. E. Intracellular quinone reduction in Sporotrichum pulverulentum by a NAD(P)H: Quinone oxidoreductase: Possible role in vanillic acid catabolism *FEBS Lett.* **1979**, 108 (1) 229–232 DOI: 10.1016/0014-5793(79)81216-8

[Crossref], [PubMed], [CAS]

25. 25.

Zhou, M.; Diwu, Z.; Panchuk-Voloshina, N.; Haugland, R. P. A stable nonfluorescent derivative of resorufin for the fluorometric determination of trace hydrogen peroxide: Applications in detecting the activity of phagocyte NADPH oxidase and other oxidases *Anal. Biochem.* **1997**, 253 (2) 162– 168 DOI: 10.1006/abio.1997.2391

[Crossref], [PubMed], [CAS]

26. 26.

King, D. W.; Cooper, W. J.; Rusak, S. A.; Peake, B. M.; Kiddle, J. J.; O'Sullivan, D. W.; Melamed, M. L.;Morgan, C. R.; Theberge, S. M. Flow injection analysis of H_2O_2 in natural waters using acridinium ester chemiluminescence: Method development and optimization using a kinetic model *Anal. Chem.* **2007**, 79 (11)4169– 4176 DOI: 10.1021/ac062228w

[ACS Full Text], [CAS]

27. 27.

Johnson, K. A.; Simpson, Z. B.; Blom, T. Global Kinetic Explorer: A new computer program for dynamic simulation and fitting of kinetic data *Anal. Biochem.* **2009**, 387 (1) 20– 29 DOI: 10.1016/j.ab.2008.12.024

[Crossref], [PubMed], [CAS]

28. 28.

Ianni, J. C. Kintecus, Windows version 3.9; **2006**.

29. 29.

Garg, S.; Jiang, C.; Miller, C. J.; Rose, A. L.; Waite, T. D. Iron redox transformations in continuously photolyzed acidic solutions containing natural organic matter: Kinetic and mechanistic insights *Environ. Sci. Technol.* **2013**, 47 (16) 9190– 9197 DOI: 10.1021/es401087q

[ACS Full Text], [CAS]

30. 30.

Pracht, J.; Boenigk, J.; Isenbeck-Schröter, M.; Keppler, F.; Schöler, H. F. Abiotic Fe(III) induced mineralization of phenolic substances *Chemosphere* **2001**, 44 (4) 613– 619 DOI: 10.1016/S0045-6535(00)00490-2

[Crossref], [PubMed], [CAS]

31. 31.

Baxendale, J.; Hardy, H. Kinetics and equilibria in solutions containing ferrous ion, ferric ion, and some substituted hydroquinones and Quinones *Trans. Faraday Soc.* **1954**, 50, 808– 814 DOI: 10.1039/tf9545000808

[Crossref], [CAS]

32. 32.

Anschutz, A. J.; Penn, R. L. Reduction of crystalline iron(III) oxyhydroxides using hydroquinone: Influence of phase and particle size *Geochem. Trans.* **2005**, 6 (3) 60– 66 DOI: 10.1186/1467-4866-6-60

[Crossref], [CAS]

33. 33.

Williams, G. R. The reduction of cytochrome c by hydroquinone *Biochem. Cell Biol.* **1963**, 41 (1) 231– 237DOI: 10.1139/o63-028

[Crossref]

34. 34.

Yamazaki, I.; Ohnishi, T. One-electron-transfer reactions in biochemical systems I. Kinetic analysis of the oxidation-reduction equilibrium between quinol-quinone and ferro-ferricytochrome c *Biochim. Biophys. Acta, Biophys. Incl. Photosynth.* **1966**, 112 (3) 469– 481 DOI: 10.1016/0926-6585(66)90249-4

[Crossref], [CAS]

35. 35.

Rich, P. R.; Bendall, D. S. A mechanism for the reduction of cytochromes by quinols in solution and its relevance to biological electron transfer reactions *FEBS Lett.* **1979**, 105 (2) 189– 194 DOI: 10.1016/0014-5793(79)80608-0

[Crossref], [PubMed], [CAS]

36. 36.

Rich, P. R.; Bendall, D. S. The kinetics and thermodynamics of the reduction of cytochrome c by substituted p-benzoquinols in solution *Biochim. Biophys. Acta, Bioenerg.* **1980**, 592 (3) 506– 518 DOI: 10.1016/0005-2728(80)90095-X

[Crossref], [PubMed], [CAS]

37. 37.

Rich, P. R. Electron transfer reactions between quinols and quinones in aqueous and aprotic media*Biochim. Biophys. Acta, Bioenerg.* **1981**, 637 (1) 28– 33 DOI: 10.1016/0005-2728(81)90206-1

[Crossref], [CAS]

38. 38.

Baxendale, J.; Hardy, H.; Sutcliffe, L. Kinetics and equilibria in the system ferrous ion+ ferric ion+ hydro-quinone+ quinone *Trans. Faraday Soc.* **1951**, 47, 963– 973 DOI: 10.1039/tf9514700963

[Crossref], [CAS]

39. 39.

Jones, A. M.; Griffin, P. J.; Waite, T. D. Ferrous iron oxidation by molecular oxygen under acidic conditions: The effect of citrate, EDTA and fulvic acid *Geochim. Cosmochim. Acta* **2015**, 160, 117– 131 DOI: 10.1016/j.gca.2015.03.026

[Crossref], [CAS]

40. 40.

Jones, A. M.; Griffin, P. J.; Collins, R. N.; Waite, T. D. Ferrous iron oxidation under acidic conditions – The effect of ferric oxide surfaces *Geochim. Cosmochim. Acta* **2014**, 145 (0) 1– 12 DOI: 10.1016/j.gca.2014.09.020

[Crossref], [CAS]

41. 41.

Li, Y.; Kuppusamy, P.; Zweier, J. L.; Trush, M. A. ESR evidence for the generation of reactive oxygen species from the copper-mediated oxidation of the benzene metabolite, hydroquinone: role in DNA damage*Chem.-Biol. Interact.* **1995**, 94 (2) 101– 120 DOI: 10.1016/0009-2797(94)03326-4

[Crossref], [PubMed], [CAS]

42. 42.

Mandal, S.; Kazmi, N. H.; Sayre, L. M. Ligand dependence in the copper-catalyzed oxidation of hydroquinones *Arch. Biochem. Biophys.* **2005**, 435 (1) 21– 31 DOI: 10.1016/j.abb.2004.11.025

[Crossref], [PubMed], [CAS]

43. 43.

Li, Y. B.; Trush, M. A. Oxidation of hydroquinone by copper: Chemical mechanism and biological effects*Arch. Biochem. Biophys.* **1993**, 300 (1) 346– 355 DOI: 10.1006/abbi.1993.1047

[Crossref], [PubMed], [CAS]

44. 44.

Li, Y. B.; Trush, M. A. DNA damage resulting from the oxidation of hydroquinone by copper: role for a Cu(II)/Cu(I) redox cycle and reactive oxygen generation *Carcinogenesis* **1993**, 14 (7) 1303– 1311 DOI: 10.1093/carcin/14.7.1303

[Crossref], [PubMed], [CAS]

45. 45.

Miller, C. J.; Vincent Lee, S. M.; Rose, A. L.; Waite, T. D. Impact of natural organic matter on H_2O_2-mediated oxidation of Fe(II) in coastal seawaters *Environ. Sci. Technol.* **2012**, 46 (20) 11078– 11085 DOI: 10.1021/es3022792

[ACS Full Text], [CAS]

46. 46.

Murphy, S. A.; Solomon, B. M.; Meng, S.; Copeland, J. M.; Shaw, T. J.; Ferry, J. L. Geochemical production of reactive oxygen species from biogeochemically reduced Fe *Environ. Sci. Technol.* **2014**, 48 (7) 3815–3821 DOI: 10.1021/es4051764

[ACS Full Text], [CAS]

47. 47.

Pignatello, J. J.; Oliveros, E.; MacKay, A. Advanced Oxidation Processes for Organic Contaminant Destruction Based on the Fenton Reaction and Related Chemistry *Crit. Rev. Environ. Sci. Technol.* **2006**, 36(1) 1– 84 DOI: 10.1080/10643380500326564

[Crossref], [CAS]

48. 48.

Miller, C. J.; Rose, A. L.; Waite, T. D. Hydroxyl radical production by H_2O_2-mediated oxidation of Fe(II) complexed by suwannee river fulvic acid under circumneutral freshwater conditions *Environ. Sci. Technol.***2013**, 47 (2) 829– 835 DOI: 10.1021/es303876h

[ACS Full Text], [CAS]

49. 49.

Bishop, C.; Tong, L. Equilibria of substituted semiquinones at high pH *J. Am. Chem. Soc.* **1965**, 87 (3) 501–505 DOI: 10.1021/ja01081a018

[ACS Full Text], [CAS]

50. 50.

Meisel, D. Free energy correlation of rate constants for electron transfer between organic systems in aqueous solutions *Chem. Phys. Lett.* **1975**, 34 (2) 263– 266 DOI: 10.1016/0009-2614(75)85269-9

[Crossref], [CAS]

51. 51.

King, D. W.; Lounsbury, H. A.; Millero, F. J. Rates and Mechanism of Fe(II) Oxidation at Nanomolar Total Iron Concentrations *Environ. Sci. Technol.* **1995**, 29 (3) 818– 824 DOI: 10.1021/es00003a033

[ACS Full Text], [CAS]

52. 52.

Rush, J. D.; Bielski, B. H. Pulse radiolytic studies of the reactions of HO2/O2 with Fe (II)/Fe (III) ions. The reactivity of HO2/O2 with ferric ions and its implication on the occurrence of the Haber-Weiss reaction *J. Phys. Chem.* **1985**, 89 (23) 5062– 5066 DOI: 10.1021/j100269a035

[ACS Full Text], [CAS]

53. 53.

Wehrli, B. Redox reactions of metal ions at mineral surfaces *Aquatic Chemical Kinetics* **1990**, 311– 336

54. 54.

Jones, A. M.; Griffin, P. J.; Collins, R. N.; Waite, T. D. Ferrous iron oxidation under acidic conditions – The effect of ferric oxide surfaces *Geochim. Cosmochim. Acta* **2014**, 145, 1– 12 DOI: 10.1016/j.gca.2014.09.020

[Crossref], [CAS]

55. 55.

Morel, F. M. M.; Hering, J. G. *Principles and Applications of Aquatic Chemistry*. Wiley: New York, **1993**.

56. 56.

Meisel, D.; Czapski, G. One-electron transfer equilibriums and redox potentials of radicals studied by pulse radiolysis *J. Phys. Chem.* **1975**, 79 (15) 1503– 1509 DOI: 10.1021/j100582a004

[ACS Full Text], [CAS]

57. 57.

Buettner, G. R. The pecking order of free-radicals and antioxidants - lipid-peroxidation, alpha-tocopherol, and ascorbate *Arch. Biochem. Biophys.* **1993**, 300 (2) 535– 543 DOI: 10.1006/abbi.1993.1074

[Crossref], [PubMed], [CAS]

58. 58.

Eyer, P. Effects of superoxide dismutase on the autoxidation of 1,4-hydroquinone *Chem.-Biol. Interact.***1991**, 80 (2) 159– 176 DOI: 10.1016/0009-2797(91)90022-Y

[Crossref], [PubMed], [CAS]

59. 59.

Ishii, T.; Fridovich, I. Dual effects of superoxide dismutase on the autoxidation of 1,4-naphthohydroquinone*Free Radical Biol. Med.* **1990**, 8 (1) 21– 24 DOI: 10.1016/0891-5849(90)90140-E

[Crossref], [PubMed], [CAS]

60. 60.

Mochizuki, M.; Yamazaki, S.-i.; Kano, K.; Ikeda, T. Kinetic analysis and mechanistic aspects of autoxidation of catechins *Biochim. Biophys. Acta, Gen. Subj.* **2002**, 1569 (1–3) 35– 44 DOI: 10.1016/S0304-4165(01)00230-6

[Crossref], [PubMed], [CAS]

61. 61.

Kalyanaraman, B.; Sealy, R. C.; Sinha, B. An electron spin resonance study of the reduction of peroxides by anthracycline semiquinones *Biochim. Biophys. Acta, Gen. Subj.* **1984**, 799 (3) 270– 275 DOI: 10.1016/0304-4165(84)90270-8

[Crossref], [PubMed], [CAS]

62. 62.

Zhu, B.-Z.; Zhao, H.-T.; Kalyanaraman, B.; Frei, B. Metal-independent production of hydroxyl radicals by halogenated quinones and hydrogen peroxide: an ESR spin trapping study *Free Radical Biol. Med.* **2002**, 32(5) 465– 473 DOI: 10.1016/S0891-5849(01)00824-3

[Crossref], [PubMed], [CAS]

63. 63.

Zafiriou, O. C. Chemistry of superoxide ion-radical (O2-) in seawater. I. pKasw* (HOO) and uncatalyzed dismutation kinetics studied by pulse radiolysis *Mar. Chem.* **1990**, 30, 31– 43 DOI: 10.1016/0304-4203(90)90060-P

[Crossref], [CAS]

64. 64.

Yuan, X.; Pham, A. N.; Xing, G.; Rose, A. L.; Waite, T. D. Effects of pH, chloride, and bicarbonate on Cu(I) oxidation kinetics at circumneutral pH *Environ. Sci. Technol.* **2012**, 46 (3) 1527– 1535 DOI: 10.1021/es203394k

[ACS Full Text], [CAS]

65. 65.

Adams, G.; Michael, B. Pulse radiolysis of benzoquinone and hydroquinone. Semiquinone formation by water elimination from trihydroxy-cyclohexadienyl radicals *Trans. Faraday Soc.* **1967**, 63, 1171– 1180 DOI: 10.1039/tf9676301171

[Crossref], [CAS]

66. 66.

Roginsky, V.; Barsukova, T. Kinetics of oxidation of hydroquinones by molecular oxygen. Effect of superoxide dismutase *J. Chem. Soc., Perkin Trans. 2* **2000**, 7) 1575– 1582 DOI: 10.1039/b000538j

[Crossref]

67. 67.

Kitagawa, S.; Fujisawa, H.; Sakurai, H. Scavenging effects of dihydric and polyhydric phenols on superoxide anion radicals, studied by electron-spin-resonance spectrometry *Chem. Pharm. Bull.* **1992**, 40 (2) 304– 307DOI: 10.1248/cpb.40.304

[Crossref], [CAS]

68. 68.

Deeble, D. J.; Parsons, B. J.; Phillips, G. O.; Schuchmann, H.-P.; Von Sonntag, C. Superoxide radical reactions in aqueous solutions of pyrogallol and N-propyl gallate: The involvement of phenoxyl radicals. A pulse radiolysis study *Int. J. Radiat. Biol.* **1988**, 54 (2) 179– 193 DOI: 10.1080/09553008814551621

[Crossref], [PubMed], [CAS]

69. 69.

Page, S. E.; Kling, G. W.; Sander, M.; Harrold, K. H.; Logan, J. R.; McNeill, K.; Cory, R. M. Dark Formation of Hydroxyl Radical in Arctic Soil and Surface Waters *Environ. Sci. Technol.* **2013**, 47 (22) 12860– 12867DOI: 10.1021/es4033265

[ACS Full Text], [CAS]

70. 70.

Buerge, I. J.; Hug, S. J. Influence of Organic Ligands on Chromium(VI) Reduction by Iron(II) *Environ. Sci. Technol.* **1998**, 32 (14) 2092– 2099 DOI: 10.1021/es970932b

[ACS Full Text], [CAS]

71. 71.

Postma, D.; Appelo, C. A. J. Reduction of Mn-oxides by ferrous iron in a flow system: column experiment and reactive transport modeling *Geochim. Cosmochim. Acta* **2000**, 64 (7) 1237– 1247 DOI: 10.1016/S0016-7037(99)00356-7

[Crossref], [CAS]

72. 72.

Borch, T.; Kretzschmar, R.; Kappler, A.; Cappellen, P. V.; Ginder-Vogel, M.; Voegelin, A.; Campbell, K.Biogeochemical Redox Processes and their Impact on Contaminant Dynamics *Environ. Sci. Technol.* **2010**,44 (1) 15– 23 DOI: 10.1021/es9026248

[ACS Full Text], [CAS]

73. 73.

Jiang, C.; Garg, S.; Waite, T. D. Hydroquinone-mediated redox cycling of iron and concomitant oxidation of hydroquinone in oxic waters under acidic conditions: Comparison with iron-natural organic matter interactions *Environ. Sci. Technol.* **2015**, 49 (24) 14076– 14084 DOI: 10.1021/acs.est.5b03189

[ACS Full Text], [CAS]